# Orientation and Microstructure Effects on Susceptibility Reconstruction: a Diffusion Phantom Study

**J. Lindemeyer[1], A-M. Oros-Peusquens[1], E. Farrher[1], F. Grinberg[1], and N. J. Shah[1,2]**
[1]Institute of Neuroscience and Medicine - 4, Forschungszentrum Juelich, Juelich, Germany, [2]Department of Neurology, Faculty of Medicine, JARA, RWTH Aachen, Aachen, Germany

**Introduction:** The reconstruction of local magnetic susceptibility in tissue is an emerging field of research. In a magnetic field, susceptibility variations give rise to characteristic $B_0$ field shifts. In inverse approaches, field shifts have been utilised successfully to reconstruct the susceptibility distribution, $\chi$ (e.g. de Rochefort [1] or Wharton [2]). These methods are primarily based on a well-accepted model describing the observed field as a convolution of $\chi$ with a dipole-shaped field. The model works well for structures that are homogeneous on the scale of the voxel size, but will most likely suffer from substructures within a voxel that produce deviant local field distortions. A prominent example for this are white matter fibre bundles that cannot be resolved with the limited voxel resolution in MRI [3,4]. Furthermore, the measured volume portion (water) is only partially representative for the content of the imaged voxel. This study investigates the behaviour of field shifts and observed susceptibility in a diffusion phantom containing a bulk of parallel straight Dyneema® fibres.

**Materials and Methods:** A straight fibre phantom [5] was measured using various angles relative to $B_0$. The phantom consists of a cylindrical, upright water container that holds the fibre model. To achieve relaxation times close to values inside the human brain, the phantom was filled with distilled water and doped with manganese sulphate in a concentration of approximately 3%. The T1 of the phantom was determined by spectroscopy to be 780ms. The fibres (consisting of Dyneema®, Ø 16µm) are densely wound around a perspex plate and compressed by two additional plates. The fibre bulk is aligned with the base and is positioned at the centre of the phantom. The susceptibility of Dyneema® is known to be different from that of water [6] and is thus optimally suited to our purpose. All experiments were performed on a Siemens TIM TRIO (3T) (Siemens Healthcare, Erlangen, Germany) MRI scanner. The phantom was rotated around its upright axis at the angles [-90°, -67.5°, -54.7°, -45°, -33.75°, -22.5°, 0°, 22.5°, 33.75°, 45°, 54.7°, 67.5°] with respect to $B_0$. At each position a multiple echo 3D gradient echo sequence was measured. A total of 32 echoes was recorded at an echo spacing of 3.38ms (starting at TE=1.6ms) with TR=110ms and an image matrix of 174x192x144 voxels (0.8mm isotropic). $B_0$ fieldmaps were computed using voxelwise unwrapping in time domain and linear regression on the phase images of the first six echoes (which globally showed sufficient SNR). The measurements were coregistered by realigning the rotation angle and by afterwards matching the transverse shifts. Two pairs of representative regions were selected to estimate a mean “fibre-area” minus “free-water” field difference. Each pair was positioned symmetrically along the vertical axis and with respect to the phantom centre. The “free-water” pair (each 43x33x16 voxels) was positioned with one region above and one region below the perspex plates. The “fibre-area” pair (each 43x33x9 voxels) was positioned between the plates. Calculation of the average difference is the best approach to obtain a representative field shift since the application of a field homogenisation algorithm is not advisable (it would also distort the field generated by the fibres which varies smoothly with position). To interpret this field difference two simulations using a simple dipole convolution were performed, each based on a model that roughly matches the geometrical structure of our phantom. Fibres were simulated a) as a bulk and b) stacked with a chequerboard cross-section. In the simulations a constant (but arbitrary) fibre susceptibility was assumed and set negative compared to that of water (this was determined by inspection). For the bulk case, the whole ROIs in the fibre area were used to calculate the field difference (as before). For the stacked fibres, only the field between the fibres was evaluated (since Dyneema® itself does not produce a signal). The susceptibility distribution inside the phantom was estimated using an algorithm based on the approach of de Rochefort [1].

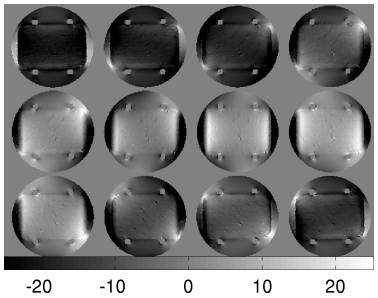


**Fig. 1:** Normalised fieldmap slice of the fibre area for all measured rotation angles (see text) in Hz

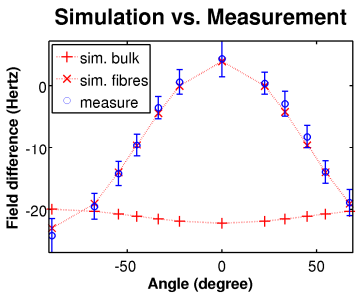


**Fig. 2:** Results of simulation and measurement in identical ROIs; error bars indicate standard deviation

**Results:** The computed field maps show large variation inside the fibre area. Due to the phantom filling process, despite careful preparation and handling, a number of small air bubbles remained between the fibres. As the bubbles are sparsely distributed, the comparatively large ROIs compensate for the bubble influences when calculating the mean. Fig. 1 shows a central slice of each measurement (angles from left to right, top to bottom as denoted above) aligned with the rotation plane, thus showing a horizontal cross section of the fibre region. Fig. 2 shows a comparison of simulation and measurement. Due to the arbitrarily chosen susceptibility value in the simulation, the simulation graphs have been scaled to match the magnitude of the measurement. Fig. 3 shows the susceptibility difference between the same ROIs in arbitrary units. Susceptibility appears to change with orientation and does not remain within the error range.

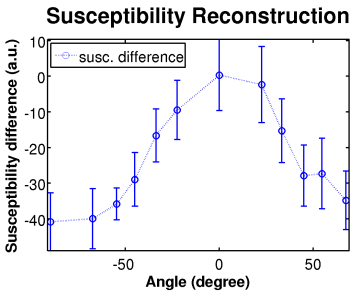


**Fig. 3:** Reconstructed average susceptibility difference (arbitrary units)

**Discussion and Perspective:** The simulation of the field caused by a homogeneous mean susceptibility shows a completely different shape compared to our measurements. The simulation of the chequerboard-stacked fibres on the other hand, exhibits an astonishing similarity when fitted to our results. Although our simulated model does not represent true fibre stacking and scales, it imitates the observed field effects convincingly. We see that macroscopic field measurements of areas containing parallel elements cannot be described by a bulk susceptibility in the corresponding region. This is an important point for susceptibility studies especially those concerning regions such as the corpus callosum, which mainly consist of parallel nerve fibres. Despite achieving convincing reconstructions in other studies, the sophisticated algorithm developed by de Rochefort was not able to deliver a conclusive result here. The apparently anisotropic susceptibility can be explained by the locally inappropriate spatial resolution which does not satisfy the underlying model (while in continuous space this would work perfectly). Thus, it is essential to be aware of structure-specific effects that might corrupt the consistency of reconstructions whenever the assumed model is violated. An anisotropy of the susceptibility of Dyneema® itself or the included diffusing water volume might play an additional role, but these influences have not been quantified in this study yet. The reconstruction of susceptibility in global consistency is one of our main goals in present and future research. This demands closer investigation of effects that might arise in brain tissue. The presented simulation approach seems to offer a convenient method to numerically estimate the field induced by the examined structure. The conclusion regarding susceptibility reconstruction is that a hybrid model including deconvolution methods as well as knowledge-based handling of particular areas might be a promising approach.

**References:**

[1] de Rochefort et al., MRM 63:194–206 (2010); [2] Wharton et al., MRM 63:1292–1304 (2010); [3] Lee et al., PNAS, 107(11):5130–5135 (2010); [4] He et al., PNAS, 106(32):13558–13563 (2009); [5] Farrher et al., Prod. Intl. Soc. Mag. Reson. Med. 18 (2010), 1640; [6] Fieremans et al., Diffusion Fundamentals 10:10.1 - 10.3 (2009)